Pergamon

PII: S0148-9062(97)00329-X

Int. J. Rock Mech. Min. Sci. Vol. 35, No. 1, pp. 43–61, 1998

Printed in Great Britain
0148-9062/98 $19.00 + 0.00

Determination of Deformability and Tensile Strength of Anisotropic Rock Using Brazilian Tests

CHAO-SHI CHEN
ERNIAN PAN
BERNARD AMADEI

This paper is the first of a series of two papers dealing with the determination of the deformability, tensile strength and fracturing of anisotropic rocks by diametral compression (Brazilian test) of discs of rock. It presents a combination of analytical and experimental methods for determining in the laboratory the elastic constants and the indirect (Brazilian) tensile strength of transversely isotropic rocks, i.e. rocks with one dominant direction of planar anisotropy. A computer program based on the complex variable function method and the generalized reduced gradient method was developed to determine the elastic constants of idealized linearly elastic, homogeneous, transversely isotropic media from the strains measured at the center of discs subjected to diametral loading. The complex variable function method was also used to construct charts for determining the indirect tensile strength of anisotropic media from the failure loads measured during diametral loading. Brazilian tests were conducted on four types of bedded sandstones assumed to be transversely isotropic. Based on strain measurements obtained with 45° strain gage rosettes glued at the center of the discs, the five independent elastic constants of the tested rocks could be determined. The elastic constants determined with the Brazilian tests were compared with those obtained from conventional uniaxial compression tests. The indirect (Brazilian) tensile strength of the tested sandstones was found to depend on the angle between the apparent planes of rock anisotropy and the direction of diametral loading. © 1998 *Elsevier Science Ltd.*

INTRODUCTION

Many rocks exposed near the Earth's surface show well-defined fabric elements in the form of bedding, stratification, layering, foliation, fissuring or jointing. In general, these rocks have properties (physical, dynamic, thermal, mechanical, hydraulic) that vary with direction and are said to be inherently *anisotropic*. Anisotropy can be found at different scales in a rock mass ranging from intact specimens to an entire rock mass. Anisotropy is a characteristic of intact foliated metamorphic rocks (slates, gneisses, phyllites, schists) and intact laminated, stratified or bedded sedimentary rocks (shales, sandstones, siltstones, limestones, coal, etc.). At a larger scale, rock mass anisotropy is found in volcanic formations (basalt, tuff), in sedimentary formations consisting of alternating layers or beds of different rock types and in rock formations cut by one or several regularly spaced joint sets.

Rock anisotropy plays an important role in various engineering activities. In civil and mining engineering, rock anisotropy affects the stability of underground excavations, surface excavations and foundations. Rock anisotropy affects drilling, blasting and rock cutting. It can also induce directional fluid flow and contaminant transport. In petroleum engineering, rock anisotropy is a critical factor in controlling borehole deviation, stability, deformation and failure. It also impacts fracturing and fracture propagation.

Despite its noted importance, rock anisotropy is still poorly understood, in particular in practice. An issue that often arises is how to characterize rock anisotropy in the laboratory and *in situ*. This paper presents a combination of experimental and analytical methods for determining in the laboratory the deformability and indirect tensile strength of intact rocks that are

University of Colorado, Department of Civil Engineering, Boulder, CO 80309-0428, U.S.A.

transversely isotropic (i.e., with one dominant direction of planar anisotropy).

In the laboratory, the mechanical properties of intact anisotropic rocks are usually determined by testing samples cut at different angles with respect to the apparent planes of anisotropy. The testing methods can be divided into static and dynamic, a review of which can be found in the recent papers of Homand *et al.* [1] and Amadei [2]. The static methods include uniaxial compression, triaxial compression, multiaxial compression, diametral compression (Brazilian test), hollow cylinder test, torsion and bending. The dynamic methods include the resonant bar method and the ultrasonic pulse method. In general, the preparation of the test specimens, their dimensions, and the minimum number of test specimens necessary to determine the properties of anisotropic rocks depend on the method used. Among these testing methods, the diametral loading of discs of rock (Brazilian test) seems to be the only method for which specimen preparation is not as stringent as with other techniques, and for which the analysis of the test results is relatively straightforward. Thus, the research presented in this paper focuses on using the Brazilian test to determine the deformability and tensile strength of anisotropic rocks.

As far as deformability is concerned, Hondros [3] used the Brazilian test method for determining the Young's modulus and Poisson's ratio of concrete assumed to be isotropic. Pinto [4] extended Hondros' method to anisotropic rocks and tested the method on discs of schist. Closed-form solutions were derived to relate the elastic constants of an anisotropic rock in a disc under diametral compression to the strains at the disc center. Pinto [4] assumed that the stress concentration at the center of a disc of anisotropic rock was the same as that for an isotropic rock. This assumption is only correct if the disc is parallel to a plane of transverse isotropy. In all other cases, however, the anisotropy needs to be taken into account. Based on correct closed-form solutions derived by Okubo [5] and Lekhnitskii [6], Amadei *et al.* [7] revised Pinto's procedure and proposed an iterative procedure to determine the five elastic constants of transversely isotropic rocks. However, the procedure did not account for the thermodynamic constraints that limit the range of variation of the elastic properties [8].

In this paper, determination of the elastic constants was obtained by solving a nonlinear system constrained by inequalities associated with thermodynamic constraints on the elastic properties [8]. Based on strains measured during Brazilian tests, the constrained system of equations can be solved using a constrained optimization technique called the generalized reduced gradient method [9, 10]. For this purpose, a computer program was developed to numerically solve this problem, and four types of sandstones were tested to get the needed experimental data. The calculated elastic constants from the proposed method were compared with those from uniaxial compression tests conducted on the same rock.

The effect of anisotropy on the indirect tensile strength of rocks determined by the Brazilian test was investigated by Berenbaum and Brodie [11] on coal, Evans [12] on coal, Hobbs [13] on siltstone, sandstone and mudstone, McLamore and Gray [14] on shale, and Barla [15] on gneiss and schist. In general, the test samples were found to fail along the loaded diameter irrespective of the orientation of the planes of rock anisotropy. The indirect tensile strength was approximated by an equation based on the theory of isotropic elasticity despite the anisotropic character of the rock. Such a method of analysis is not correct since the stress distribution in an anisotropic disc can be expected to differ from that in an isotropic disc.

Lekhnitskii [6] used the complex stress function method to express the relation between stresses and strains within a thin disc of anisotropic material under diametrical loading. The application of this method to measure the tensile strength of anisotropic rocks was demonstrated by Amadei and Jonsson [16] and Chen *et al.* [17]. In this paper, charts are proposed to determine the indirect tensile strength of anisotropic rocks. Brazilian tests were conducted on discs of two types of sandstones assumed to be transversely isotropic. The variation of the sandstone indirect tensile strength with the inclination angle between the apparent rock layers (plane of transverse isotropy) and the applied diametral load was also investigated. Note that throughout this paper, compressive stresses and contractile strains are taken as positive.

THEORETICAL BACKGROUND

Elastic equilibrium of an anisotropic disc subjected to diametral loading

Consider a thin disc of a linearly elastic, homogeneous, continuous, and transversely isotropic medium with the geometry of Fig. 1. The disc has a thickness, t, and a diameter $D = 2R$. Let x, y, z be a global Cartesian coordinate system with the z-axis

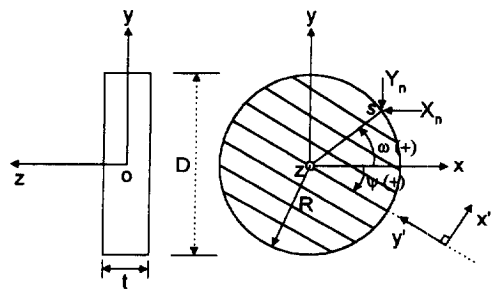

Fig. 1. Problem geometry. Anisotropic disc loaded by surface tractions with components X_n and Y_n.

defining the longitudinal axis of the disc, and let X_n, Y_n be the components in the x and y directions of surface forces per unit area (i.e., the given tractions) acting along the edge of the disc. The surface forces are assumed to be in equilibrium. A local coordinate system x', y', z' is attached to the plane of transverse isotropy of the medium such that the x'-axis is normal to the plane, the y'- and z'-axes are contained within the plane and the z'-axis coincides with the z-axis. The angle ψ is defined as the inclination angle between the plane of transverse isotropy and the x-axis.

If it can be assumed (i) that the disc has a plane of elastic symmetry parallel to its middle plane, (ii) that the disc is loaded by surface forces that vary negligibly across its thickness and (iii) that deformation of the disc is small, then a generalized plane stress formulation can be used [6]. In this formulation, if the equations of equilibrium for stress, the compatibility equations for strain, the strain displacement relations, the constitutive relations and the boundary conditions are all expressed in terms of average values of stress, strain and displacement across the disc thickness, then it can be shown that the mean stress components (σ_x, σ_y, τ_{xy}), the mean strain components (ε_x, ε_y, γ_{xy}) and the mean displacement components satisfy the same equations that govern the classical plane strain formulation in the x–y plane [6]. The only difference is that the constitutive relation of the material in the x–y plane is expressed as follows:

$$\begin{Bmatrix} \varepsilon_x \\ \varepsilon_y \\ \gamma_{xy} \end{Bmatrix} = \begin{bmatrix} a_{11} & a_{12} & a_{16} \\ a_{12} & a_{22} & a_{26} \\ a_{16} & a_{26} & a_{66} \end{bmatrix} \cdot \begin{Bmatrix} \sigma_x \\ \sigma_y \\ \tau_{xy} \end{Bmatrix} \tag{1}$$

where a_{11}, a_{12}, ..., a_{66} are the compliance components calculated in the x, y coordinate system. These components depend on the angle ψ and the elastic constants in the x', y', z' coordinate system. For a transversely isotropic medium, the number of independent constants is equal to five. Throughout this paper, the constants are called E, E', ν, ν' and G' such that E and E' are the Young's moduli in the plane of transverse isotropy and in a direction normal to it, respectively; ν and ν' are the Poisson's ratios characterizing the lateral strain response in the plane of transverse isotropy to a stress acting parallel and normal to it, respectively; and G' is the shear modulus in planes normal to the plane of transverse isotropy. The shear modulus G in the plane of transverse isotropy is not independent and is equal to $E/(2(1+\nu))$. Using coordinate transformation rules, it can be shown that for the geometry of Fig. 1, a_{11}, a_{12}, ..., a_{66} are independent of ν and are related to E, E', ν' and G' as follows [2]

$$\begin{aligned}
a_{11} &= \frac{\sin^4\psi}{E'} + \frac{\cos^4\psi}{E} + \frac{\sin^2 2\psi}{4}\left(\frac{1}{G'} - \frac{2\nu'}{E'}\right) \\
a_{12} &= \frac{\sin^2 2\psi}{4}\left(\frac{1}{E'} + \frac{1}{E} - \frac{1}{G'}\right) - \frac{\nu'}{E'}(\cos^4\psi + \sin^4\psi) \\
a_{16} &= \sin 2\psi\left[\left(\frac{\sin^2\psi}{E'} - \frac{\cos^2\psi}{E}\right) + \left(\frac{1}{2G'} - \frac{\nu'}{E'}\right)\cos 2\psi\right] \\
a_{22} &= \frac{\cos^4\psi}{E'} + \frac{\sin^4\psi}{E} + \frac{\sin^2 2\psi}{4}\left(\frac{1}{G'} - \frac{2\nu'}{E'}\right) \\
a_{26} &= \sin 2\psi\left[\left(\frac{\cos^2\psi}{E'} - \frac{\sin^2\psi}{E}\right) - \left(\frac{1}{2G'} - \frac{\nu'}{E'}\right)\cos 2\psi\right] \\
a_{66} &= \sin^2 2\psi\left(\frac{1}{E'} + \frac{1}{E} + \frac{2\nu'}{E'}\right) + \frac{\cos^2 2\psi}{G'}.
\end{aligned} \tag{2}$$

Let F be a stress function such that

$$\sigma_x = \frac{\partial^2 F}{\partial y^2}, \qquad \sigma_y = \frac{\partial^2 F}{\partial x^2}, \qquad \tau_{xy} = -\frac{\partial^2 F}{\partial x \partial y}. \tag{3}$$

Substituting Equations (1) and (3) into the equation of compatibility that the strains ε_x, ε_y and γ_{xy} must satisfy yields the following differential equation:

$$a_{22}\frac{\partial^4 F}{\partial x^4} - 2a_{26}\frac{\partial^4 F}{\partial x^3 \partial y} + (2a_{12} + a_{66})\frac{\partial^4 F}{\partial x^2 \partial y^2} - 2a_{16}\frac{\partial^4 F}{\partial x \partial y^3} + a_{11}\frac{\partial^4 F}{\partial y^4} = 0. \tag{4}$$

The general solution of this equation depends on the roots, μ_i ($i = 1$–4), of its characteristic equation,

$$a_{11}\mu^4 - 2a_{16}\mu^3 + (2a_{12} + a_{66})\mu^2 - 2a_{26}\mu + a_{22} = 0. \tag{5}$$

Lekhnitskii [6] has shown that the roots of Equation (5) are always either complex or purely imaginary, two of them being the conjugate of the two others. Let μ_1, μ_2 be those roots and $\bar{\mu}_1$, $\bar{\mu}_2$ their respective conjugates. The roots μ_1 and μ_2 are also assumed to be distinct. Substituting Equation (2) into Equation (5), it can be shown that for a transversely isotropic disc and a given value of the dip angle, ψ, of the plane of transverse isotropy, the roots depend on E/E', E/G' and ν'.

As shown by Lekhnitskii [6], the first derivatives of F with respect to x and y can be expressed as

$$\begin{aligned}
\frac{\partial F}{\partial x} &= 2\mathrm{Re}[\phi_1(z_1) + \phi_2(z_2)], \\
\frac{\partial F}{\partial y} &= 2\mathrm{Re}[\mu_1\phi_1(z_1) + \mu_2\phi_2(z_2)],
\end{aligned} \tag{6}$$

where $\phi_k(z_k)$ ($k = 1, 2$) are analytic functions of the complex variables $z_k = x + \mu_k y$ and Re denotes the real part of the complex expression in the brackets. Combining Equations (3) and (6), we obtain the general expression for the stress components

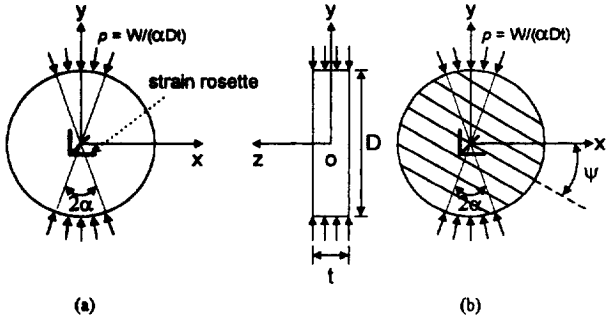

Fig. 2. Diametral compression of a thin disc over an angular width of 2α. (a) Loading in the plane of transverse isotropy, (b) loading in the plane perpendicular to the plane of transverse isotropy.

$$\sigma_x = 2\mathrm{Re}[\mu_1^2\phi_1'(z_1) + \mu_2^2\phi_2'(z_2)],$$
$$\sigma_y = 2\mathrm{Re}[\phi_1'(z_1) + \phi_2'(z_2)]$$
$$\tau_{xy} = -2\mathrm{Re}[\mu_1\phi_1'(z_1) + \mu_2\phi_2'(z_2)], \qquad (7)$$

where $\phi_k'(z_k)$ $(k = 1, 2)$ are the first derivatives of $\phi_k(z_k)$ with respect to z_k. In addition to Equation (4), the stress function F must satisfy the boundary conditions along the outer contour of the disc, which take the form

$$2\mathrm{Re}(\phi_1 + \phi_2) = -\int_0^s Y_n ds,$$
$$2\mathrm{Re}(\mu_1\phi_1 + \mu_2\phi_2) = \int_0^s X_n ds, \qquad (8)$$

where s is the arc length along the contour of the disc (Fig. 1). Let X_n and Y_n be expanded as Fourier series in $\cos(m\omega)$ and $\sin(m\omega)$, where m varies between 1 and an arbitrary number N and ω is an angle defined in Fig. 1 which varies between 0 and 2π. After integration, Equation (8) becomes

$$2\mathrm{Re}(\phi_1 + \phi_2) = \sum_{m=1}^{N}(a_m e^{im\omega} + \bar{a}_m e^{-im\omega}),$$
$$2\mathrm{Re}(\mu_1\phi_1 + \mu_2\phi_2) = \sum_{m=1}^{N}(b_m e^{im\omega} + \bar{b}_m e^{-im\omega}) \qquad (9)$$

where a_m, b_m and their respective conjugates $\bar{a}_m$, $\bar{b}_m$ are related to the coefficients of the Fourier series for X_n and Y_n [6, 7].

General expressions for the functions $\phi_1(z_1)$ and $\phi_2(z_2)$ were proposed by Lekhnitskii [6] as follows

$$\phi_1(z_1) = A_1 z_1 + \sum_{m=2}^{N} A_m p_{1m}(z_1),$$
$$\phi_2(z_2) = B_1 z_2 + \sum_{m=2}^{N} B_m p_{2m}(z_2) \qquad (10)$$

with

$$p_{km}(z_k) = \frac{-1}{(1 - i\mu_k)^m}\left[\left(\frac{z_k}{R} + \sqrt{\left(\frac{z_k}{R}\right)^2 - 1 - \mu_k^2}\right)^m + \left(\frac{z_k}{R} - \sqrt{\left(\frac{z_k}{R}\right)^2 - 1 - \mu_k^2}\right)^m\right], \quad (k = 1, 2)$$

The coefficients A_m and B_m and their conjugates can be expressed in terms of a_m, b_m, $\bar{a}_m$, $\bar{b}_m$ $(m = 2, N)$ by substituting Equation (10) into Equation (9) with $z_k/R = \cos\omega + \mu_k \sin\omega$. Then, substituting the expressions for the derivatives of $\phi_k(z_k)$ into Equation (7), the stress components σ_x, σ_y and τ_{xy} can be computed at any point (x, y) in the disc. In these components, the contribution of $A_1 z_1$ and $B_1 z_2$ consists of constant quantities that are either function of a_1 and $\bar{a}_1$, or of b_1 and $\bar{b}_1$.

Consider a uniform radial pressure $\sigma_r = p$ applied over the arcs $\pi/2 - \alpha < \omega < \pi/2 + \alpha$ and $3\pi/2 - \alpha < \omega < 3\pi/2 + \alpha$, as shown in Fig. 2. This stress distribution can be approximated by the following Fourier series in the angle ω

$$\sigma_r = A_0 + \sum_{n=1}^{N-1}(A_n \cos n\omega + B_n \sin n\omega) \qquad (11)$$

with

$$A_0 = 2p\alpha/\pi, \qquad A_n = \frac{2p}{\pi}\left(\frac{1 + (-1)^n}{n}\right)\cos\frac{n\pi}{2}\sin n\alpha,$$
$$B_n = 0. \qquad (12)$$

For this boundary condition, there is no shear stress applied along the contour of the disc. The surface tractions X_n, Y_n depend on p only, and can then be expressed as Fourier series in $\cos(m\omega)$ and $\sin(m\omega)$, with m varying between 1 and N.

The loading angle 2α is assumed to be small such that p is equal to $W/(\alpha Dt)$ where W is the load (force) applied on the disc in the y direction. For the boundary conditions defined by Equations (11) and (12), it can be shown that at any point (x, y) within the disc, the components of the stress field can be written as follows [7]

$$\sigma_x = \frac{W}{\pi Dt} q_{xx}, \qquad \sigma_y = \frac{W}{\pi Dt} q_{yy}, \qquad \tau_{xy} = \frac{W}{\pi Dt} q_{xy} \qquad (13)$$

where q_{xx}, q_{yy} and q_{xy} are three stress concentration factors that depend on the coordinates (x, y) of the point of interest, the loading angle 2α, and the compliance components a_{11}, a_{12}, a_{22}, a_{16}, a_{26} and a_{66}. In view of Equation (2), the stress concentration factors depend on the dip angle ψ and the ratios of elastic constants E/E', E/G' and ν'. Substituting Equation (13) into Equation (1) yields

$$\frac{\pi Dt}{W}\begin{Bmatrix}\varepsilon_x\\ \varepsilon_y\\ \gamma_{xy}\end{Bmatrix}=\begin{bmatrix}a_{11} & a_{12} & a_{16}\\ a_{21} & a_{22} & a_{26}\\ a_{16} & a_{26} & a_{66}\end{bmatrix}\cdot\begin{Bmatrix}q_{xx}\\ q_{yy}\\ q_{xy}\end{Bmatrix}. \quad (14)$$

Stress distribution in a disc under diametral loading

A computer program was developed to determine the stresses at any arbitrary point in a disc of transversely isotropic medium under diametral loading. In the following analysis, the applied load W is assumed to be uniformly distributed over a strip of angle $2\alpha = 15°$ (see Fig. 2) and the disc diameter-to-thickness ratio D/t is equal to 2 (as recommended by ISRM [23]). Figure 3(a–c) show respectively the distribution of the dimensionless stress components $\sigma_x/(W/\pi Dt) = q_{xx}$, $\sigma_y/(W/\pi Dt) = q_{yy}$ and $\tau_{xy}/(W/\pi Dt) = q_{xy}$ over the disc surface for the isotropic case or when the disc is cut parallel to a plane of transverse isotropy (Fig. 2(a)). In both cases, $E/E' = 1$, $\nu' = \nu = 0.25$ and $E/G' = E/G = 2(1 + \nu) = 2.5$. The calculated values of q_{xx}, q_{yy} and q_{xy} at the center of the disc are -1.96 (≈ -2), 5.96 (≈ 6) and 0, respectively.

In order to assess the role played by anisotropy on the stress distribution, consider the geometry of Fig. 2(b) where the plane of transverse isotropy is now perpendicular to the disc surface and is assumed to dip at an angle ψ. The values of $\sigma_x/(W/\pi Dt) = q_{xx}$, $\sigma_y/(W/\pi Dt) = q_{yy}$ and $\tau_{xy}/(W/\pi Dt) = q_{xy}$ were determined at different points over the disc surface for $E/E' = 3$, $E/G' = 7.5$, $\nu' = 0.25$ and $\psi = 45°$. The distribution of the dimensionless stress components is shown in Fig. 4(a–c). Contours of dimensionless in-plane principal stresses $\sigma_1/(W/\pi Dt)$ and $\sigma_3/(W/\pi Dt)$ (with $\sigma_1 > \sigma_3$) for $\psi = 0°$, 45° and 90° are illustrated in Fig. 5. Several conclusions can be drawn from Figs 3–5.

(1) The stress distribution near the center of a disc under diametral loading is quite uniform for both isotropic and anisotropic cases. The stress distribution in the y direction is more uniform than in the x direction.

(2) Determination of the stresses at the disc center from strain gage measurements requires that the strain gages be small with a length not exceeding 10% of the diameter of the disc.

(3) Compared to the isotropic solution, both the anisotropic character and the inclination angle ψ of the plane of anisotropy have a strong influence on the magnitude of the stresses in the disc.

(4) In the anisotropic case, the stress contours are not symmetric with respect to the x and y axes except when $\psi = 0°$ and 90°.

(5) Fig. 5(a and c) ($\psi = 0°$ and 90°) show that the in-plane principal stresses σ_1 and σ_3 along the loaded diameter are parallel to the y and x axes, respectively. However, the same observation can not be made when $\psi = 45°$ (Fig. 5(b)). In that case, σ_1 is inclined at an angle with respect to the loading diameter. For the example shown here, it appears that the angle does not exceed 5°. This implies that, unless $\psi = 0°$ or 90°, the shear stress is, in general, not zero along the loaded diameter for anisotropic discs.

(6) The maximum tensile stress (max. σ_3) is located at the center of the disc. This means that the initiation of fracture during diametral loading will be at the center of the disc if a fracture criterion of maximum principal stress is adopted.

Determination of the elastic constants of transversely isotropic media

As mentioned earlier, the deformability of a transversely isotropic medium is characterized by five independent elastic constants which we called E, E', ν, ν' and G' in the x', y', z' coordinate system of Fig. 1. The previous theory can be applied to determine those five constants from strains measured at the center of two conveniently oriented discs under diametral loading as shown in Fig. 2(a and b).

(1) One disc, whose middle plane is parallel to the plane of transverse isotropy of the medium (Fig. 2(a)), is used to determine the isotropic constants E and ν. For this orientation, the variation of the stress concentration factors q_{xx}, q_{yy} and q_{xy} with the half-loading strip angle α is shown in Fig. 6. This figure indicates that for small values of the angle α ($\alpha \leq 7.5°$), the stress concentration factors at the center of the disc can be approximated by $q_{xx} = -2$, $q_{yy} = 6$ and $q_{xy} = 0$ (which are the conventional values used for the analysis of Brazilian tests on isotropic media). Then, Equation (14) can be written as follows:

$$\frac{\pi Dt}{W}\begin{Bmatrix}\varepsilon_x\\ \varepsilon_y\\ \gamma_{xy}\end{Bmatrix}=\begin{bmatrix}1/E & -\nu/E & 0\\ -\nu/E & 1/E & 0\\ 0 & 0 & 2(1+\nu)/E\end{bmatrix}\cdot\begin{Bmatrix}-2\\ 6\\ 0\end{Bmatrix}. \quad (15)$$

By measuring the longitudinal strain on the disc surface in at least two nonparallel directions, Equation (15) can be solved for both E and ν.

(2) One disc, whose middle plane is perpendicular to the plane of transverse isotropy of the medium (Fig. 2(b)), is used to determine E', ν' and G'. For this orientation, it can be shown that Equation (14) can be written as follows:

$$\frac{\pi Dt}{W}\begin{Bmatrix}\varepsilon_x\\ \varepsilon_y\\ \gamma_{xy}\end{Bmatrix}-\frac{1}{E}\begin{Bmatrix}C_1\\ C_2\\ C_3\end{Bmatrix}=\begin{bmatrix}T_{11} & T_{12} & T_{13}\\ T_{21} & T_{22} & T_{23}\\ T_{31} & T_{32} & T_{33}\end{bmatrix}\cdot\begin{Bmatrix}1/E'\\ \nu'/E'\\ 1/G'\end{Bmatrix}, \quad (16)$$

where C_1, C_2, C_3, T_{11}, ..., T_{33} depend on q_{xx}, q_{yy}, q_{xy} and the angle ψ. In selecting the elastic constants for a transversely isotropic medium, the following thermodynamic constraints must be satisfied [8, 18]

$$E, E', G \text{ and } G' > 0; \qquad 1 - \nu - 2\frac{E}{E'}(\nu')^2 > 0 \quad (17)$$

Equation (16) is a highly nonlinear system with three unknowns ($1/E'$, ν'/E' and $1/G'$) which are

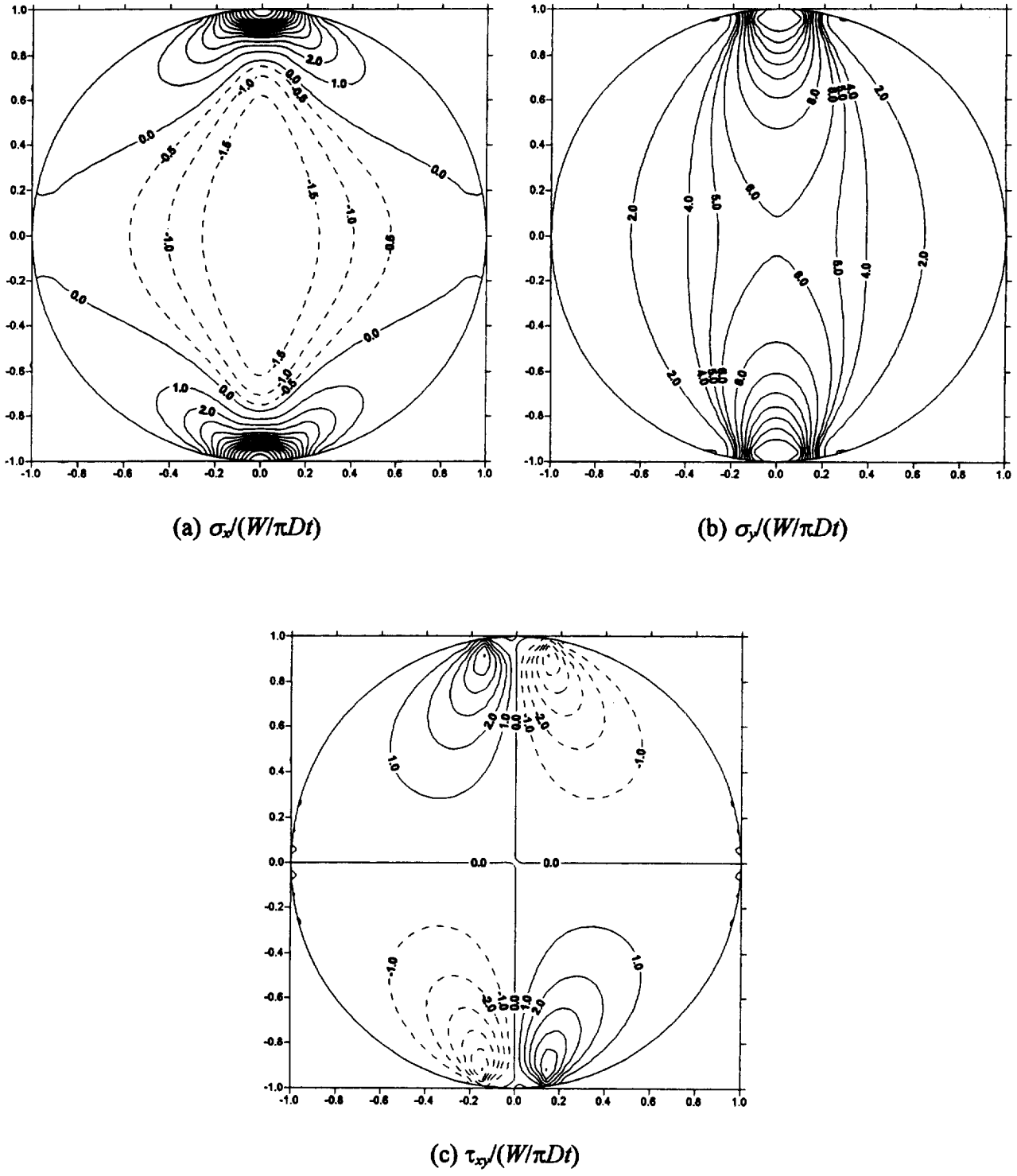

Fig. 3. Distribution of $\sigma_x/(W/\pi Dt) = q_{xx}$, $\sigma_y/(W/\pi Dt) = q_{yy}$ and $\tau_{xy}/(W/\pi Dt) = q_{xy}$ in (a), (b) and (c), respectively. Isotropic case.

constrained by the inequalities in Equation (17). This system can be solved using a constrained optimization technique called the generalized reduced gradient (GRG) method [9, 10]. The steps in the GRG algorithm can be found in Abadie [19]. In this study, a computer program based on the GRG method was developed to numerically solve the nonlinear constrained optimization problem represented by Equations (16) and (17). The problem is solved for the three unknown elastic constants E', ν' and G' which, when combined with E and ν, completely describe the deformability of the tested material.

The aforementioned methodology requires that the disc specimens be cut in specific directions with respect to the plane of transverse isotropy of the material being investigated. Therefore, it implies that the orien-

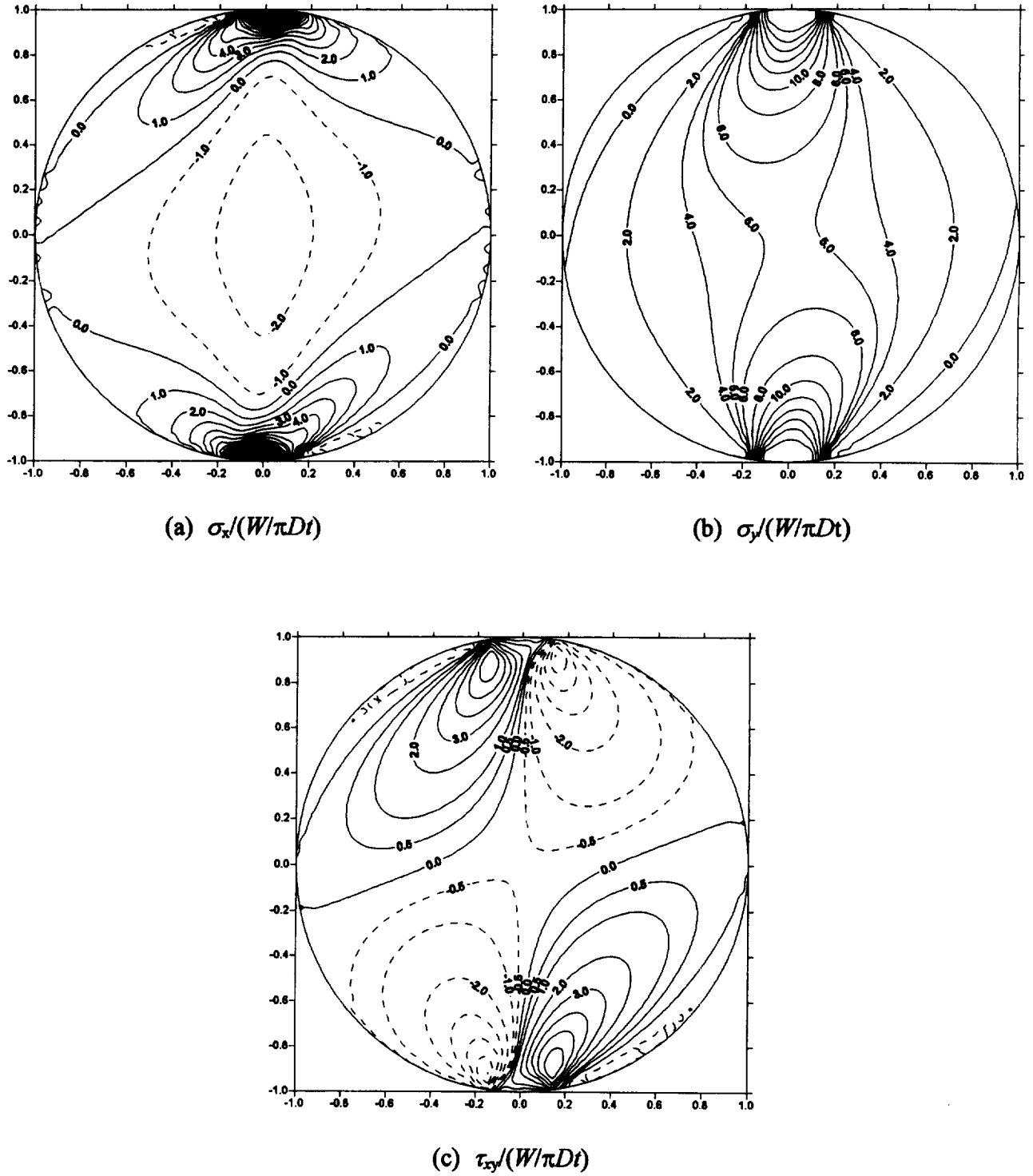

Fig. 4. Distribution of $\sigma_x/(W/\pi Dt) = q_{xx}$, $\sigma_y/(W/\pi Dt) = q_{yy}$ and $\tau_{xy}/(W/\pi Dt) = q_{xy}$ in (a), (b) and (c), respectively. Transversely isotropic case with $E/E' = 3$, $E/G' = 7.5$, $\nu' = 0.25$, and $\psi = 45°$.

tation of the material anisotropy be known beforehand.

EXPERIMENTAL INVESTIGATION

The deformability and tensile strength of four types of bedded sandstones referred to as types I, II, III and IV below, were determined as part of this study. Large blocks of type I and type II sandstones (Loveland sandstone) were purchased from the Colorado Stone Company near Boulder, CO. A large block of type III sandstone originated from the Boulder Creek, West of Boulder. Records of experiments conducted on type IV sandstone by Jonsson [20] were also used in this study. In general, all four sandstones consisted of hard silica-cemented quartzose showing slight metamorphosis.

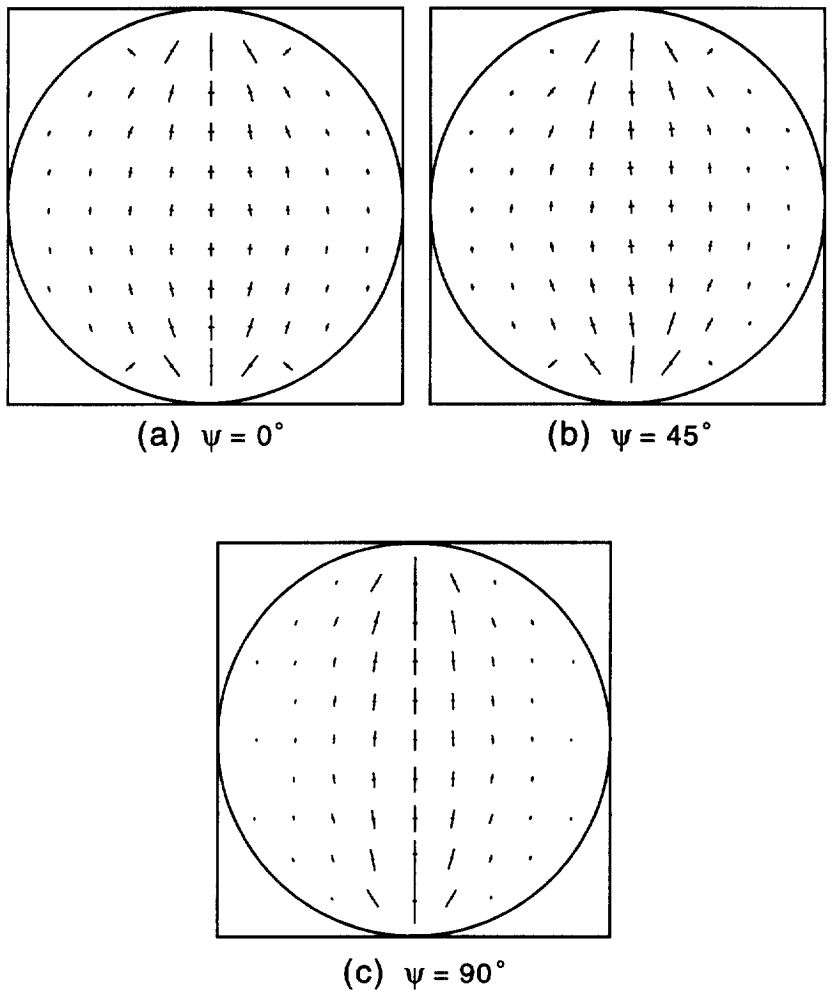

Fig. 5. Distribution of dimensionless principal stresses $\sigma_1/(W/\pi Dt)$ and $\sigma_3/(W/\pi Dt)$ (with $\sigma_1 > \sigma_3$). (a) $\psi = 0°$; (b) $\psi = 45°$; (c) $\psi = 90°$.

Because the sandstones exhibited many thin and parallel layers, they were all assumed to be transversely isotropic with the plane of transverse isotropy taken parallel to the apparent direction of rock symmetry. The elastic constants of the four sandstones were determined by conducting uniaxial compression tests and Brazilian tests on the same rock. All the test specimens were cored in the laboratory at selected orientations from the blocks of rock. The cores were NX-size with a diameter D = 2.14 in. (54.4 mm) and were prepared to give specimens with a length-to-diameter ratio, L/D, of 2.0 for the uniaxial compression tests, and a thickness-to-diameter ratio, t/D, of 0.5 for the Brazilian tests.

Uniaxial compression tests

As shown by Amadei [2, 21], the five elastic constants of a rock modeled as a transversely isotropic medium can be determined by uniaxial compression of at least three specimens, cut at different angles to the plane of transverse isotropy. Figure 7 shows the configuration of the uniaxial compression tests conducted in this study. The load was applied in the y (vertical) direction and strains were measured in the x, y and z directions. In Fig. 7, the angle, θ_a, defines the dip angle of the plane of transverse isotropy of the rock.

Three groups of specimens of each sandstone were tested. The strains measured on the specimens with $\theta_a = 0°$ (group a in Fig. 7(a)) allowed the determination of E' and ν' whereas those on the specimens with $\theta_a = 90°$ (group b in Fig. 7(b)) were used to determine E and ν. Finally, the strains measured on the specimens with $\theta_a \neq 0°$ or 90° (group c in Fig. 7(c)) were used to determine the shear modulus G'. To measure the strains, two pairs of 45° strain gage rosettes were mounted on planes parallel to the x-axis for the group a specimens, and four 45° strain gage rosettes were attached on planes parallel to the x- and z-axes for the group b and group c specimens. All the strain gages (type EA-06-060RZ-120) had a length of 3 mm and a resistance of 120 Ω, and were glued in the middle section of the specimens.

A computer program based on the least square method was written to efficiently determine the five elastic constants of each rock based on the strains measured in the uniaxial compression tests. Let N be the total number of longitudinal strain measurements (with $N \geq 5$) obtained for all specimens of a given rock

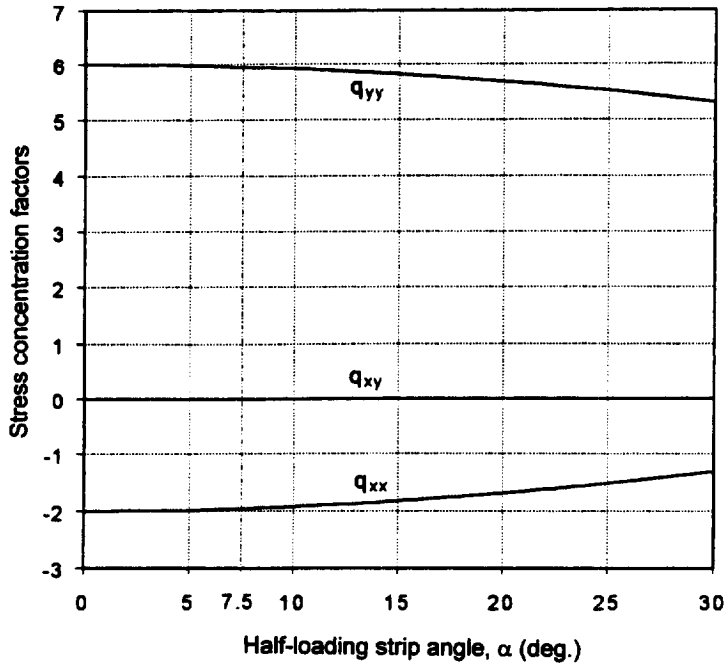

Fig. 6. Variation of stress concentration factors q_{xx}, q_{yy} and q_{xy} with the half-loading strip angle α. Loading in the plane of transverse isotropy or isotropic case.

(groups a to c). As shown by Amadei [2] (see Equations (13) and (14), pp. 299), each strain measurement is linearly related to the five unknown compliances $1/E$, $1/E'$, ν/E, ν'/E' and $1/G'$. In matrix form, the strain measurements can then be expressed in terms of the five compliances as follows:

$$\{\varepsilon\} = [T]\begin{Bmatrix} 1/E \\ 1/E' \\ \nu/E \\ \nu'/E' \\ 1/G' \end{Bmatrix} \tag{18}$$

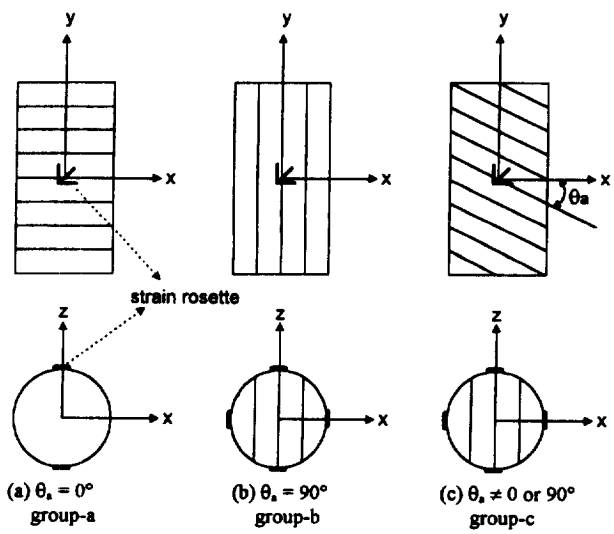

Fig. 7. Three groups of rock specimens tested in uniaxial compression with (a) $\theta_a = 0°$, group a; (b) $\theta_a = 90°$, group b; (c) $\theta_a \neq 0$ or 90°, group c.

where $\{\varepsilon\}$ is a $(N \times 1)$ matrix of strain measurements and $[T]$ is a $(N \times 5)$ matrix related to the angle θ_a. Equation (18) is then solved for the least square (best fit) estimate of the five compliance terms by multilinear regression analysis. The advantage of this approach is that all strain measurements are taken into account when determining the compliance terms. Furthermore, the method can be extended to more than three specimens.

In this study, a total of 21 uniaxial compression tests were conducted. Table 1 gives the specimen length, L, the number of strain gage rosettes on each rock specimen and the values of the dip angle θ_a. All tests were carried out by using a MTS machine with a load capacity of 100 kips (450 kN) and at a constant loading rate of 450 lb/s (2 kN/s). Two cycles of loading and unloading were performed to ascertain the rock elastic behavior. All specimens were loaded up to failure, and the primary failure loads were recorded. Specimen preparation and loading were conducted in accordance with the ISRM suggested methods [22].

Brazilian tests

Discs of the four sandstone types were prepared following the ISRM suggested methods [23]. The end faces of the discs were flat to within 5×10^{-4} in. (0.01 mm) and parallel to within 0.25°. As recommended by the ISRM [23], two curved steel jaws were inserted between the discs and the platens of the loading frame in order to apply a strip load instead of a line load. A typewriter film ribbon was placed between the jaws and each disc to measure the contact angle, 2α, of Fig. 2. Based

Table 1. Sandstone specimens tested in uniaxial compression

Rock type	Sample	θ_a (deg.)	No. of strain rosettes	L (in.)	Comp. strength (10^3 psi)
I	CBDX-1	0	2	4.32	18.9
	CBDX-2	0	2	4.27	24.2
	CBDI-1	24	4	4.37	13.5
	CBDI-2	24	4	4.20	14.0
	CBDZ-1	90	4	4.34	18.9
	CBDZ-2	90	4	4.23	16.9
II	UDA-1	0	2	4.29	12.3
	UDA-2	0	2	4.34	12.3
	UDC63-1	63.5	4	4.24	3.8
	UDB-1	90	4	4.50	6.6
	UDB-2	90	4	4.34	10.8
III	CB1-1	0	2	4.15	10.7
	CB3-1	0	2	4.40	12.6
	CB7-1	42.5	4	4.29	10.2
	CB7-2	39	4	4.23	11.9
	CB5-1	90	4	4.28	16.5
	CB6-1	90	4	4.26	13.2
IV*	X-1	0	3	4.02	25.5
	X-2	0	3	3.87	25.7
	Z20-1	20	3	3.91	25.6
	Z-1	90	3	4.16	27.9

*From Jonsson [20] (1 in = 25.4 mm; 10^3 psi = 6.89 MPa).

on measurements, an average contact angle of 15° was adopted for all calculations in this study. A 45° strain gage rosette with 3 mm long strain gages was glued at the center of each disc. After preparation, all specimens were loaded up to failure at a constant loading rate of 45 lb/s (0.2 kN/s) by using the same MTS loading system as in the uniaxial compression tests.

The procedure used to determine the elastic constants of each one of the four sandstones by diametral loading was as follows:

(1) Two sets of disc specimens were prepared. One set of specimens, cored normal to (or with middle plane parallel to) the plane of transverse isotropy (Fig. 2(a)), was used to calculate the isotropic constants E and ν. Another set of specimens, cored parallel to (or with middle plane perpendicular to) the plane of transverse isotropy (Fig. 2(b)), was used to determine the other three constants E', ν' and G'.

(2) The longitudinal strains in the vertical, horizontal and 45° directions were measured by gluing a 45° strain gage rosette at the center of each disc specimen.

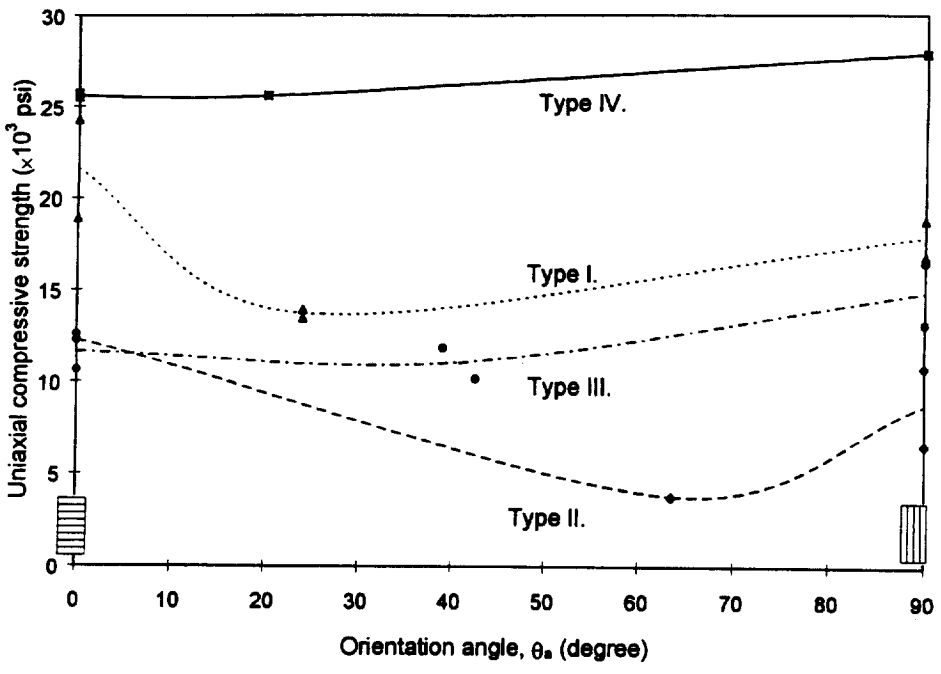

Fig. 8. Variation of the uniaxial compressive strength with the orientation angle θ_a.

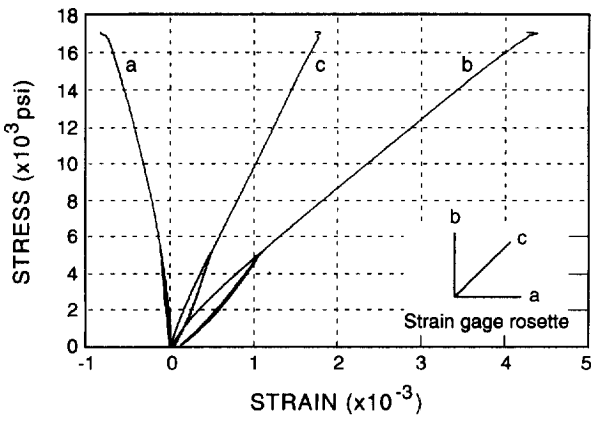

Fig. 9. Typical stress–strain curves of sample CBDZ-2 tested under uniaxial compression.

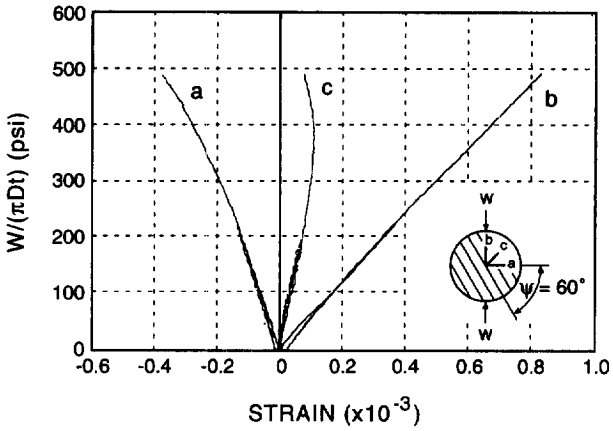

Fig. 10. Typical stress–strain curves of sample BDBZ60-1 tested under diametral compression. Strains measured with three strain gages glued to a disc with plane perpendicular to the plane of transverse isotropy.

Table 2. Average elastic constants from uniaxial compression and Brazilian tests

Rock type	Test method and No. of tests	E (×10^6 psi)	E' (×10^6 psi)	ν	ν'	G (×10^6 psi)	G' (×10^6 psi)	E/E'	G/G'
I	uniaxial comp. (6)	4.78	6.38	0.083	0.130	2.21	2.74	0.75	0.81
	Brazilian test (6)	6.18	7.84	0.080	0.136	2.86	3.56	0.79	0.80
II	uniaxial comp. (5)	4.19	3.41	0.185	0.130	1.77	0.88	1.23	2.00
	Brazilian test (9)	4.12	3.56	0.133	0.128	1.82	1.79	1.16	1.02
III	uniaxial comp. (6)	6.79	3.58	0.103	0.118	3.08	2.29	1.90	1.34
	Brazilian test (6)	7.53	7.35	0.167	0.115	3.23	2.83	1.02	1.14
IV	uniaxial comp. (4)	7.46	6.33	0.187	0.156	3.14	2.65	1.18	1.19
	Brazilian test (8)	5.06	5.20	0.270	0.358	1.99	2.40	0.97	0.83

(10^6 psi = 6.89 GPa).

Table 3. Measured strains and calculated values of E, ν and G for discs cored normal to (or with middle plane parallel to) the plane of transverse isotropy

Rock type	Sample	D (in.)	t (in.)	$\varepsilon_a\pi Dt/W$ (×10^{-6})	$\varepsilon_b\pi Dt/W$ (×10^{-6})	E (×10^6 psi)	ν	G (×10^6 psi)	$W_f/\pi Dt$ (psi)
I	BDX1	2.14	1.09	−0.39	0.97	6.37	0.078	2.95	764
	BDX2	2.14	0.98	−0.28	0.80	7.56	0.022	3.70	1014
	BDX3	2.14	1.14	−0.42	1.03	5.99	0.081	2.77	948
II	BDBX-1	2.14	1.03	−0.77	1.68	3.74	0.146	1.63	581
	BDBX-2	2.14	0.91	−0.61	1.39	4.51	0.121	2.01	584
III	BX-3	2.14	1.06	−0.39	0.79	8.04	0.182	3.40	735
	BX-5	2.14	1.14	−0.45	0.93	6.84	0.178	2.90	701
	BX-6	2.14	1.06	−0.37	0.81	7.73	0.142	3.39	755
IV	X-1	2.14	–	−0.85	1.38	4.86	0.349	1.80	650
	X-2	2.14	–	−0.61	1.39	4.48	0.120	2.00	700
	X-3	2.14	–	−0.37	0.76	7.64	0.135	3.36	740
	X-4	2.14	–	−0.62	1.07	6.17	0.298	2.38	715
	X-5	2.14	–	−0.81	1.39	4.75	0.309	1.81	725

*ε_a and ε_b represent the strains in the x and y directions of Fig. 2, respectively. (1 in = 25.4 mm; 10^6 psi = 6.89 GPa)

Table 4. Measured strains and calculated values of E', ν' and G' for discs cored parallel to (or with middle plane perpendicular to) the plane of transverse isotropy (type II sandstone)

Sample	D (in.)	t (in.)	ψ (deg.)	$\varepsilon_a\pi Dt/W$ (×10^{-6})	$\varepsilon_b\pi Dt/W$ (×10^{-6})	$\varepsilon_c\pi Dt/W$ (×10^{-6})	E' (×10^6 psi)	ν'	G' (×10^6 psi)
BCBZ00-2	2.14	1.04	0	−0.67	1.65	0.49	3.67	0.105	1.73
BCBZ15-1	2.14	1.00	15	−0.63	1.52	0.49	3.96	0.100	1.96
BDBZ30-1	2.14	1.01	30	−0.76	1.77	0.55	3.32	0.110	1.58
BDBZ45-1	2.14	1.06	45	−0.71	1.67	0.59	3.24	0.161	1.70
BDBZ60-1	2.14	1.03	60	−0.62	1.53	0.35	3.00	0.178	2.07
BDBZ75-1	2.14	0.98	75	−0.69	1.54	0.44	3.86	0.114	1.78
BCBZ90-1	2.14	0.98	90	−0.70	1.56	0.44	3.90	0.130	1.69
Average							3.56	0.128	1.79

*ε_a, ε_b and ε_c represent the strains in the x, y and 45° directions of Fig. 2, respectively. (1 in = 25.4 mm; 10^6 psi = 6.89 GPa).

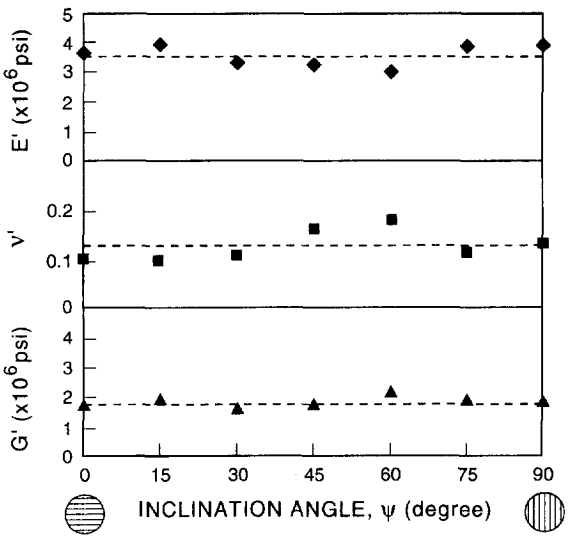

Fig. 11. Variation of E', ν' and G' with the inclination angle ψ for type II sandstone.

(3) Two steel-loading jaws were designed to apply a diametral load to each disc specimen over an arc of contact angle 2α.

(4) Each disc specimen was loaded in the vertical direction up to failure.

(5) The five elastic constants were determined from the strain gage measurements by using Equations (15)–(17).

Once the five elastic constants were determined, the tensile strength, σ_t, of each sandstone was also calculated by recording the failure load, W_f, during the Brazilian tests and by using the expression of σ_x (horizontal stress) in Equation (13); this assumption seems to be adequate in view of observations made earlier in this paper with regard to the stress distributions in Figs 3–5.

DEFORMABILITY TEST RESULTS

Uniaxial compression tests

The results of the uniaxial compression tests on the four sandstone types are reported in Table 1. Figure 8 shows the variation of the uniaxial compressive strength with the dip angle, θ_a, of the plane of transverse isotropy. This figure indicates that the maximum compressive strength occurs when the load is applied in the direction normal to the plane of transverse isotropy ($\theta_a = 0°$) for the type I and II sandstones, and occurs when $\theta_a = 90°$ for the type III and IV sandstones.

Typical response curves for sample CBDZ-2 tested under uniaxial compression are shown in Fig. 9. From the stress–strain curves, the strains measured at 50% of the ultimate strength were used in the determination of the elastic constants. Table 2 gives the secant elastic constants for the four sandstones calculated by the least square method (Equation (18)) as well as the number of tests. The values of E/E' for type II, III and IV sandstones are greater than 1, which means that for those rocks, the deformability in the direction normal to their bedding is greater than that parallel to their bedding. However, an opposite observation was found for type I sandstone.

Brazilian tests

Typical response curves for sample BDBZ60-1 tested under diametral loading are shown in Fig. 10. Based on the strains measured at 50% of the ultimate stresses, the five elastic constants of the four sandstones were determined by diametral loading on two sets of samples. The first set was loaded in the plane of transverse isotropy (Fig. 2(a)). Since in the experiments, the contact angle 2α never exceeded 15°, and in view of Fig. 6, the stress concentration factors in Equation (13) were approximated by $q_{xx} = -2$, $q_{yy} = 6$ and $q_{xy} = 0$. Table 3 gives the specimen sizes, the values of the measured strains, the failure stress ($W_f/\pi Dt$), and the calculated values of E and ν. In this table, ε_a and ε_b represent the strains measured in the x (horizontal) and y (vertical) directions, respectively.

The second set of samples was loaded in the plane perpendicular to the plane of transverse isotropy (Fig. 2(b)). Table 4 gives the specimen sizes, the values of the measured strains and the calculated values of E', ν' and G' for type II sandstone.

The average values of the five elastic constants determined from the uniaxial compression and Brazilian tests are compared in Table 2. For each type of sandstone, differences in some of the elastic constants can be noted. For instance, for type I sandstone, the moduli determined under diametral loading are consistently higher (by about 20–30%) than those determined under uniaxial compression; however, the ratios E/E' and G/G' are similar for both testing methods. For type IV sandstone, the E/E' and G/G' ratios are less than unity for the Brazilian test and larger than unity for the uniaxial compression test. Further, the value of G obtained with the Brazilian test is much smaller (by about 35%) than that determined under uniaxial compression. For type II sandstone, the value of G' was found to be much smaller under uniaxial compression than under diametral loading. This could be explained by an inherent defect clearly visible in the cylindrical specimen subjected to uniaxial compression. For type III sandstone, the value of E' was found to be smaller under uniaxial compression than under diametral loading. No apparent reason could be found for this discrepancy. Because most of the values of E/E' for the four rock types range between 1 and 2, the sandstones can be classified as moderately anisotropic rocks.

The three elastic constants E', ν' and G' of type II sandstone were determined by diametral loading of disc specimens with layers dipping at different angles, ψ, with respect to the horizontal (see Fig. 2(b)). Figure 11 shows values of the three elastic constants for ψ = 0°, 15°, 30°, 45°, 60°, 75° and 90°. The dotted

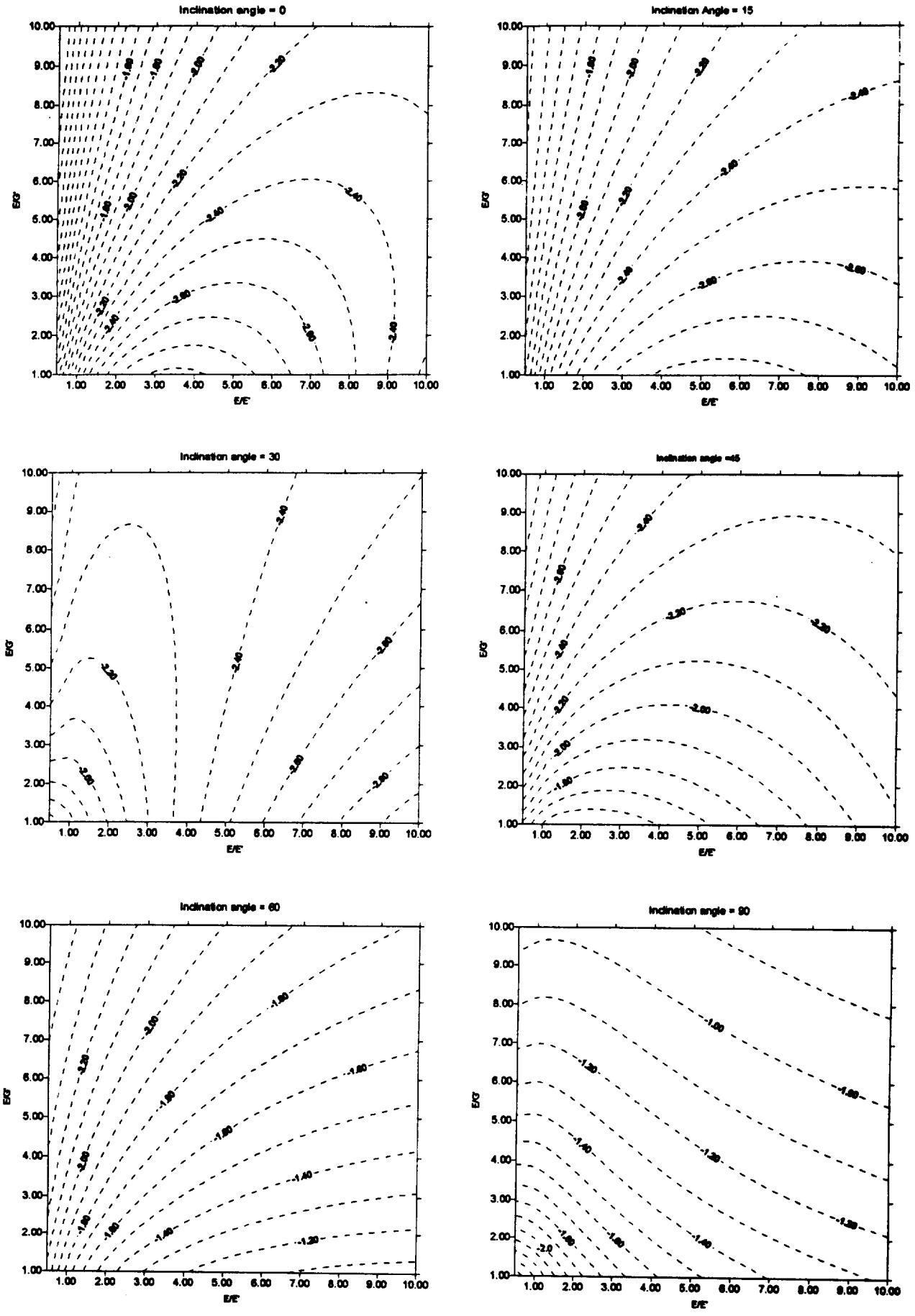

Fig. 12. Variation of stress concentration factor q_{xx} for various values of E/E', E/G' and the inclination angle ψ and for $\nu' = 0.1$. The isotropic case corresponds to $E/E' = 1$ and $E/G' = 2.2$.

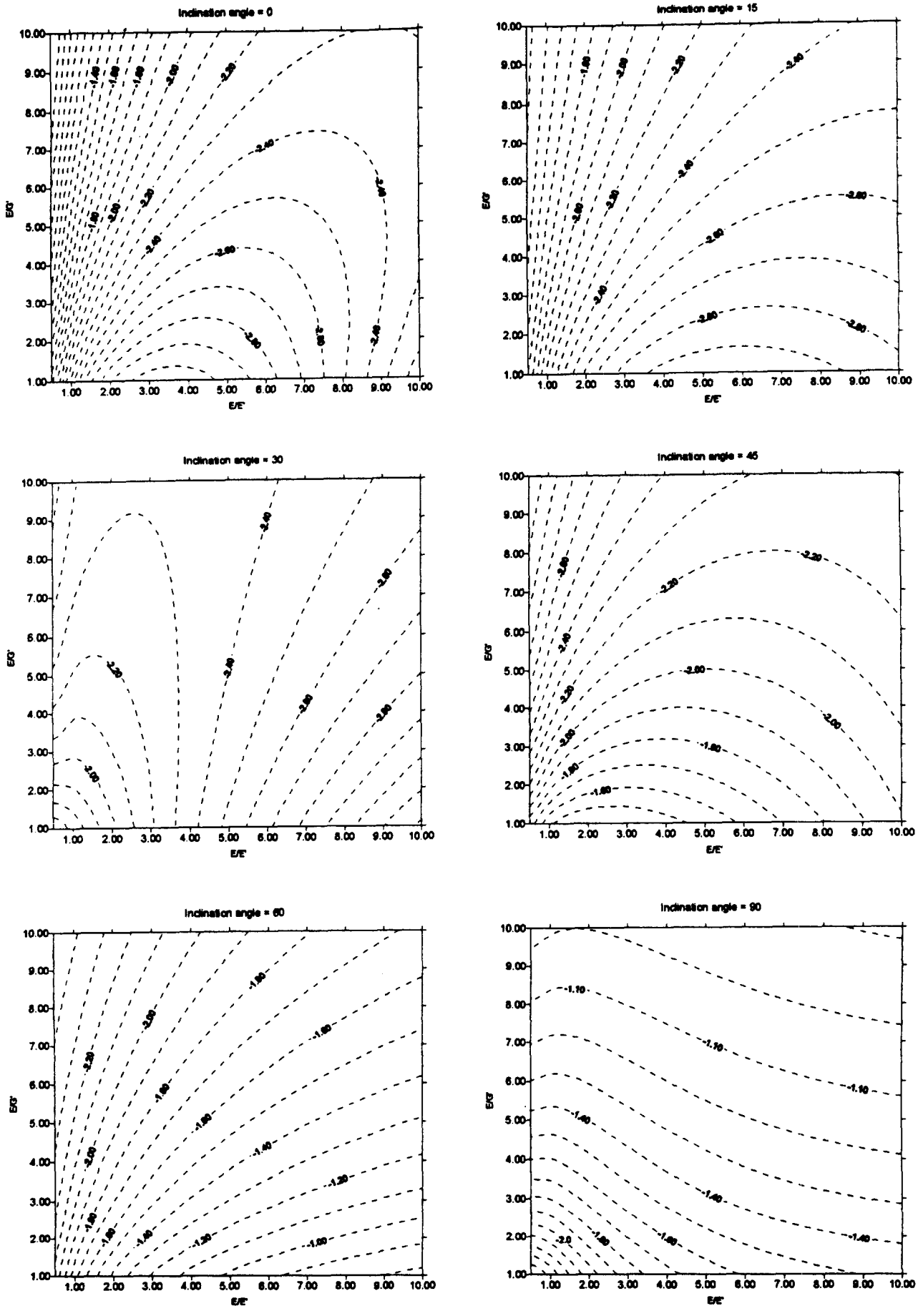

Fig. 13. Variation of stress concentration factor q_{xx} for various values of E/E', E/G' and the inclination angle ψ and for $\nu' = 0.2$. The isotropic case corresponds to $E/E' = 1$ and $E/G' = 2.4$.

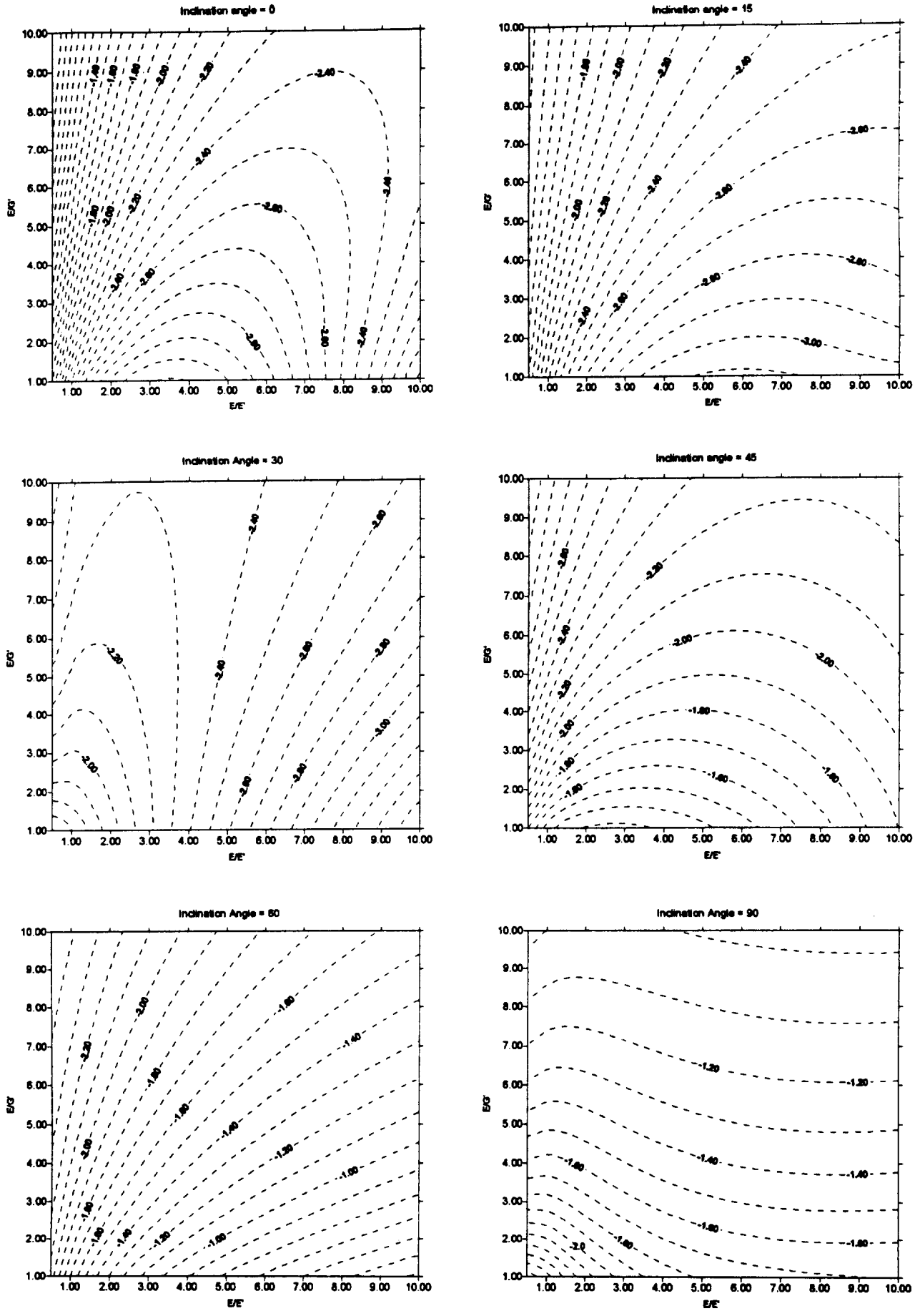

Fig. 14. Variation of stress concentration factor q_{xx} for various values of E/E', E/G' and the inclination angle ψ and for $\nu' = 0.3$. The isotropic case corresponds to $E/E' = 1$ and $E/G' = 2.6$.

Table 5. Brazilian test results on type I and type II sandstones

Rock type	Sample	D (in.)	t (in.)	ψ (deg.)	W_f (10^3 lbf)	$W_f/\pi Dt$ (10^3 psi)	Failure mode*
Type I.	Z2-2	2.14	1.08	0	5.53	0.76	T
	Z1-1	2.14	1.00	15	5.04	0.75	T
	Z1-2	2.14	1.05	30	5.32	0.75	T
	Z1-3	2.14	1.02	45	5.85	0.85	T
	Z1-4	2.14	1.05	60	4.25	0.60	T&S
	Z1-7	2.14	1.09	67.5	4.30	0.59	S
	Z1-5	2.14	1.02	75	3.84	0.56	S
	Z2-1	2.14	1.02	90	5.50	0.80	T
Type II.	BCBZ00-2	2.14	1.04	0	2.59	0.37	T
	BCBZ15-1	2.14	1.00	15	3.19	0.47	T
	BDBZ30-1	2.14	1.01	30	4.26	0.63	T
	BDBZ45-1	2.14	1.06	45	3.52	0.50	T
	BDBZ60-1	2.14	1.03	60	3.39	0.49	T
	BDBZ75-1	2.14	0.98	75	0.92	0.14	S
	BCBZ90-1	2.14	0.98	90	2.43	0.37	T

*T = tensile failure mode, S = shear failure mode. (1 in = 25.4 mm; 10^3 lbf = 4.45 kN; 10^3 psi = 6.89 MPa).

lines in that figure represent the average values of the elastic constants, i.e. $E' = 3.6 \times 10^6$ psi (25 GPa), $\nu' = 0.128$, and $G' = 1.8 \times 10^6$ psi (12.5 GPa). Figure 11 shows a limited amount of scatter around the average values, which for all practical purposes, is acceptable for the type of material under consideration. The test results also indicate that the transversely isotropic model is reasonable for the sandstone.

TENSILE STRENGTH TEST RESULTS

As shown in Equation (13), the stress state at each point (x, y) of the disc can be expressed by three components σ_x, σ_y and τ_{xy} which depend on the stress concentration factors q_{xx}, q_{yy} and q_{xy}, respectively. The stress distributions of Figs 3 and 4 clearly show that for points along the loaded diameter, σ_x is tensile and constant over most of the diameter, σ_y is compressive and varies along the diameter and τ_{xy} is not zero (unless $\psi = 0°$ or 90°). The nonvanishing character of τ_{xy} implies that, in general, the principal stresses along the loaded diameter are inclined with respect to the x- and y-axes. However, as shown by Amadei *et al.* [7] and as confirmed in this study, the inclination angle does not seem to exceed 5°.

Thus, if we make the assumption that the indirect tensile strength, σ_t, of an anisotropic rock is given by the maximum absolute value of the stress, σ_x, perpendicular to the loaded diameter at the center of the disc, then

$$\sigma_t = -q_{xx}\frac{W_f}{\pi Dt}, \tag{19}$$

where W_f is the applied load when the specimen fails; D and t are the diameter and thickness of the disc specimen; and q_{xx} is the stress concentration factor determined at $x = y = 0$. In general, q_{xx} cannot be determined using simple mathematical expressions since, as described in the previous section, it is a complex function of E/E', E/G', ν' and the material orientation angle ψ. Figures 12–14 show the variation of q_{xx} for different values of E/E', E/G', ν' and the angle ψ. These figures can be used as charts to determine q_{xx} once E, E', ν', G' and ψ are known (note that q_{xx} is independent of ν). Figures 12–14 also show that using $q_{xx} = -2$ (which corresponds to the isotropic case) for anisotropic media is erroneous.

A total of 15 Brazilian tests were conducted on discs of type I and type II sandstones in order to determine their tensile strength. The rock layers were inclined at different angles ψ ranging between 0° (horizontal layers) and 90° (vertical layers). Table 5 gives the thickness t, the inclination angle ψ, the failure load W_f, and the mode of failure for each test. A set of disc specimens of type I sandstone after failure is shown in Fig. 15. Two major modes of failure were observed: (i) tensile splitting along the loaded diameter was the dominant mode of failure when ψ varied between 0 and 60° or was equal to 90°, (ii) shear failure along the sandstone layers with or without branching was domi-

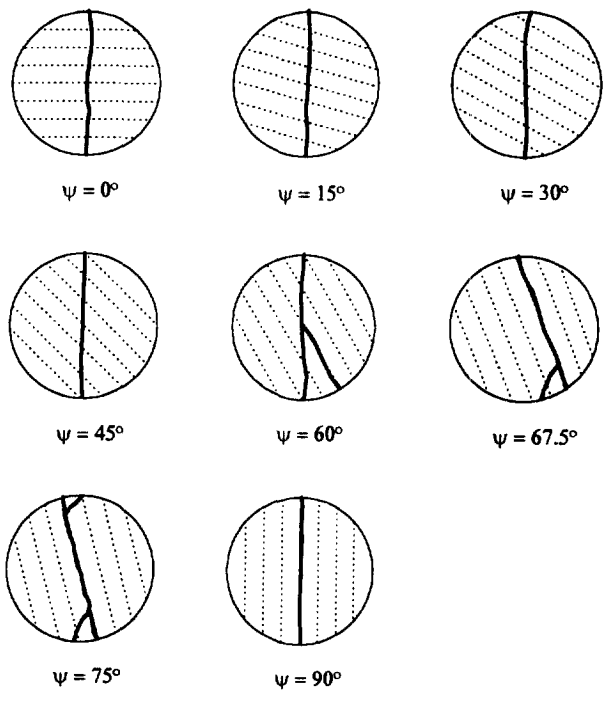

Fig. 15. Failure mode under diametral loading for different values of ψ (type I sandstone).

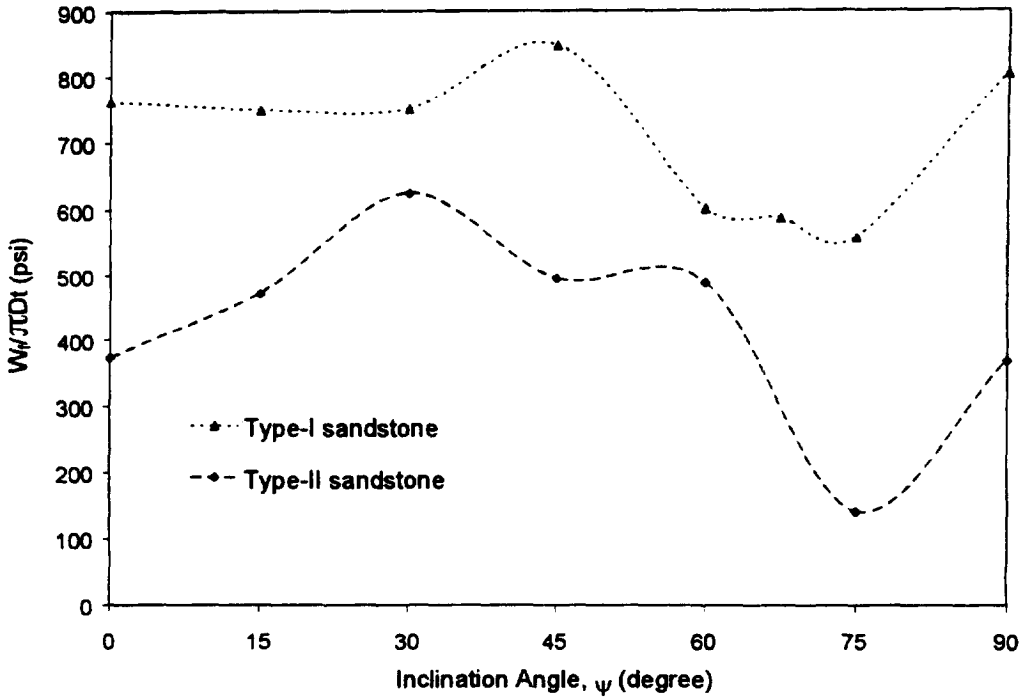

Fig. 16. Variation of the failure stress, $W_f/\pi Dt$, with the inclination angle ψ for type I and type II sandstones.

nant when ψ ranged between 60 and 90°. Mixed tensile splitting and shear was also observed in certain cases such as that shown in Fig. 15 for $\psi = 60°$.

The variation of the failure stress, $W_f/(\pi Dt)$, with the inclination angle ψ is plotted in Fig. 16. The failure stress reaches a minimum when $\psi = 75°$ for both sandstones, which seems to be consistent with the experimental results of Barla [15] on schist. The maximum failure stress occurs when $\psi = 45°$ for type I sandstone and when $\psi = 30°$ for type II sandstone.

The stress concentration factor q_{xx} was calculated using the average elastic properties listed in Table 2 and for those values of the dip angle ψ for which tensile splitting had been observed. Table 6 gives the values of q_{xx} and the tensile strength determined using Equation (19) for type I and II sandstones. The variation of q_{xx} with the angle ψ is plotted in Fig. 17 for both sandstones. This figure indicates that the stress concentration factor of −2 (the solid line) expected for the isotropic case is no longer appropriate for anisotropic media.

CONCLUSION

This paper shows that the diametral (Brazilian) loading of discs of rocks is indeed a valuable and attractive testing method for determining the deformability and tensile strength of isotropic as well as anisotropic rocks. The tests can be carried out on specimens of rocks of different sizes. Furthermore, the specimen preparation is not as stringent as with other conventional rock mechanics testing methods. The analysis of the test results is straightforward for isotropic media but requires more complex analytical and numerical tools if anisotropy needs to be taken into account. In general, this study indicates that isotropic elastic solutions cannot and should not be used for the analysis of tests on anisotropic rocks.

In this paper, an analytical procedure was presented to determine the deformability and tensile strength of anisotropic rocks from the results of Brazilian tests. The procedure assumes that the rock can be modeled as a linearly elastic, homogeneous, transversely isotropic continuum. Four types of sandstones (defined as

Table 6. Variation of q_{xx} and tensile strength for type I and type II sandstones

	$-q_{xx}$		Tensile strength σ_t (10^3 psi)	
ψ (deg.)	type I	type II	type I	type II
0	1.89	2.05	1.44	0.76
15	1.87	2.02	1.40	0.96
30	1.84	1.96	1.38	1.23
45	1.87	1.91	1.59	0.95
60	1.97	1.89	1.19	0.92
75	2.09	1.89	–	–
90	2.14	1.90	1.72	0.70

(10^3 psi = 6.89 MPa).

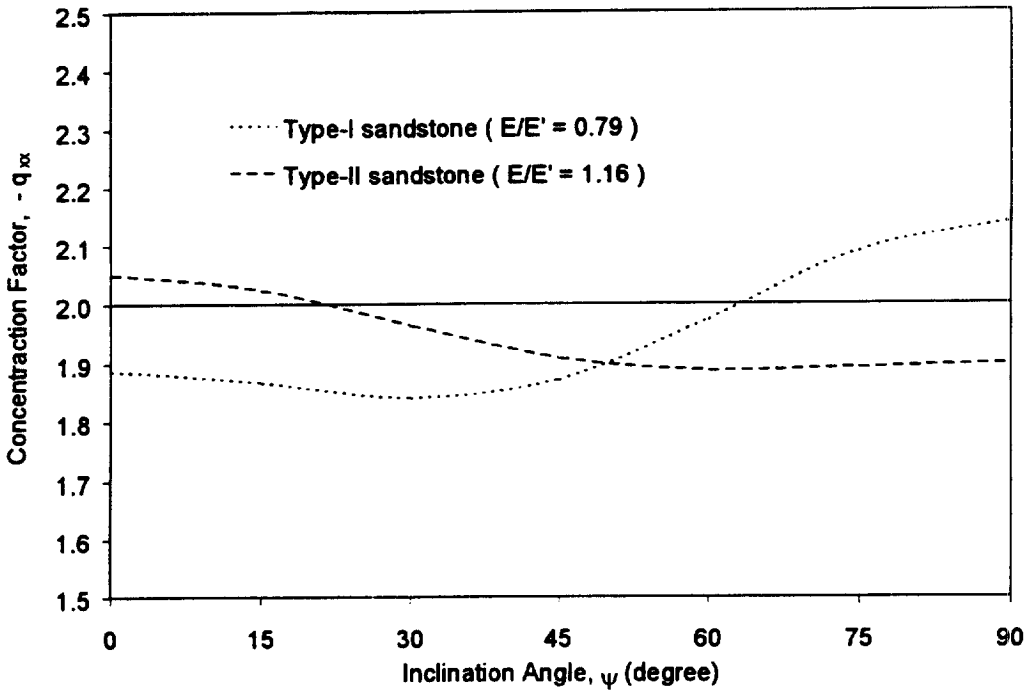

Fig. 17. Variation of q_{xx} with the inclination angle ψ for type I and type II sandstones. The isotropic case corresponding to $q_{xx} = -2$ is shown as a solid line.

type I, II, III and IV) assumed to be transversely isotropic were selected and tested. Their deformability and indirect tensile strength were determined by using the proposed Brazilian testing method. The elastic constants determined with the Brazilian tests were compared with those obtained from uniaxial compression tests conducted on the same rocks. Although the elastic constants are of the same order of magnitude for both testing methods, differences in some (but not all) elastic constants could be noted. In addition, it was found that the stress distribution near the center of a disc under diametral loading is quite uniform for both isotropic and anisotropic media. Therefore, the proposed Brazilian testing method is deemed to be a good and effective method for determining the deformability of anisotropic rocks due to its simplicity of sample preparation and test procedure. Two disc samples cut at different angles with respect to the planes of rock anisotropy are adequate to determine all of the independent constants of elasticity for transversely isotropic rocks.

The indirect tensile strength of anisotropic rocks can be determined by diametral loading of a rock disc if the assumption can be made that the tensile strength is equal to the absolute value of the maximum tensile stress acting across the loaded diameter and at the center of the disc. This applies as long as the disc fails by tensile splitting but not in shear or with any shear failure component. Determination of tensile strength requires the calculation of a stress concentration factor q_{xx} calculated at the center of the disc. When the rock is isotropic or the testing disc is cored perpendicular to a plane of transverse isotropy, the value of q_{xx} can be approximated as being equal to -2. For anisotropic rocks, however, the expression of q_{xx} is more complex and depends on analytical functions of complex variables which themselves depend on the rock elastic constants, the contact angle over which the diametral load is applied and the inclination angle of the planes of rock anisotropy. Because of the complexity of determining the value of q_{xx}, some convenient charts (Figs 12–14) were generated to determine the value of q_{xx}. Thus, in general, the tensile strength of anisotropic rocks is not a constant, but depends on the angle between the apparent planes of rock anisotropy and the direction of loading.

Acknowledgements—This research is funded in part by National Science Foundation, under grant MS-9215397.

Accepted for publication 8 November 1997

REFERENCES

1. Homand, F., Morel, E. and Henry, J.-P., Characterization of the moduli of elasticity of an anisotropic rock using dynamic and static method. *Int. J. Rock Mech. Min. Sci. Geomech. Abstr.*, 1993, **30**, 527–535.
2. Amadei, B., Importance of anisotropy when estimating and measuring *in situ* stresses in rock. *Int. J. Rock Mech. Min. Sci. Geomech. Abstr.*, 1996, **33**, 293–325.
3. Hondros, G., The evaluation of Poisson's ratio and modulus of materials of a low tensile resistance by the Brazilian (indirect tensile) test with particular reference to concrete. *J. Appl. Sci.*, 1959, **10**, 243–268.
4. Pinto, J. L., Determination of the elastic constants of anisotropic bodies by diametral compression tests. *Proc. 4th ISRM Cong.*, Montreux, Vol. 2, 1979, pp. 359–363.
5. Okubo, H., The stress distribution in an aelotropic circular disc compressed diametrically. *J. Math. Physics*, 1952, **31**, 75–83.

6. Lekhnitskii, S. G., *Anisotropic Plates* (S. W. Tsai, Trans.). Gorden and Breach, New York, 1957.
7. Amadei, B., Rogers, J. D. and Goodman, R. E., Elastic constants and tensile strength of the anisotropic rocks. *Proc. 5th ISRM Congr.*, Melbourne, A189-A196, 1983.
8. Lempriere, B. M., Poisson's ratios in orthotropic materials. *J. Am. Inst. Aeronaut. Astronaut.*, 1968, **6**, 2226–2227.
9. Chen, C. S., Characterization of Deformability, Strength, and Fracturing of Anisotropic Rocks Using Brazilian Tests. Ph.D. thesis, Dept. of Civil Eng., University of Colorado, Boulder, 1996.
10. Gabriele, G. A., Application of the Reduced Gradient Method to Optimal Engineering Design. M.Sc. thesis, School of Mechanical Eng., Purdue University, 1975.
11. Berenbaum, R. and Brodie, I., The tensile strength of coal. *J. Inst. Fuel.*, 1959, **32**, 320–327.
12. Evans, I., The tensile strength of coal. *Colliery Eng.*, 1961, **38**, 428–434.
13. Hobbs, D. W., The strength and stress–strain characteristics of coal in triaxial compression. *J. Geol.*, 1964, **72**, 214–231.
14. McLamore, R. and Gray, K. E., The mechanical behavior of anisotropic sedimentary rocks. *J. Eng. Ind.*, 1967, **89**, 62–76.
15. Barla, G., Rock anisotropy: Theory and laboratory testing, *Rock Mechanics*, ed. L. Müller. Springer-Verlag, New York, 1974, pp. 132–169.
16. Amadei, B. and Jonsson, T., Tensile strength of anisotropic rocks measured with the splitting tension test. *Proc. 12th Southeastern Conf. Theoret. Appl. Mech.*, 1984, pp. 152–159.
17. Chen, C. S., Pan, E. and Amadei, B., Evaluation of properties of anisotropic rocks using Brazilian tests. *Proc. 2nd NARMS*, Montreal, Vol. 2, 1996, pp. 1651–1658.
18. Amadei, B., Savage, W. Z. and Swolfs, H. S., Gravitational stresses in anisotropic rock masses. *Int. J. Rock Mech. Min. Sci. Geomech. Abstr.*, 1987, **24**, 5–14.
19. Abadie, J. *Integer and Nonlinear Programming: Application of the GRG Algorithm to Optimal Control Problems.* Elsevier Publ., 1970, pp. 191–211.
20. Jonsson, T., Measurements of the Deformability and Tensile Strength of Anisotropic Rock by Diametral Compression Tests. M.Sc. thesis, Dept. of Civil Eng., University of Colorado, Boulder, 1983.
21. Amadei, B., *Rock Anisotropy and the Theory of Stress Measurements.* Springer-Verlag, New York (1983).
22. Bieniawski, Z. T.*et al.*, Suggested methods for determining uniaxial compressive strength and deformability of rock materials. *Int. J. Rock Mech. Min. Sci. Geomech. Abstr.*, 1979, **16**, 135–140.
23. Bieniawski, Z. T. and Hawkes, I., Suggested methods for determining tensile strength of rock materials. *Int. J. Rock Mech. Min. Sci. Geomech. Abstr.*, 1978, **15**, 99–103.